Letter

Many-body quantum chaos in mixtures of multiple species

Vijay Kumar and Dibyendu Roy
Raman Research Institute, Bangalore 560080, India

(Received 17 October 2023; accepted 15 February 2024; published 18 March 2024)

We study spectral correlations in many-body quantum mixtures of fermions, bosons, and qubits with periodically kicked spreading and mixing of species. We take two types of mixing, namely, Jaynes-Cummings and Rabi, respectively, satisfying and breaking the conservation of a total number of species. We analytically derive the generating Hamiltonians whose spectral properties determine the spectral form factor in the leading order. We further analyze the system-size (L) scaling of Thouless time t^*, beyond which the spectral form factor follows the prediction of random matrix theory. The L dependence of t^* crosses over from $\ln L$ to L^2 with an increasing Jaynes-Cummings mixing between qubits and fermions or bosons in a finite-size chain, and it finally settles to $t^* \propto \mathcal{O}(L^2)$ in the thermodynamic limit for any mixing strength. The Rabi mixing between qubits and fermions leads to $t^* \propto \mathcal{O}(\ln L)$, previously predicted for single species of qubits or fermions without total-number conservation.

DOI: 10.1103/PhysRevE.109.L032201

A series of recent microscopic studies has explored quantum chaos and spectral correlations in periodically driven (Floquet) many-body systems [1–17] to show the emergence of a universal random matrix theory (RMT) description of the spectral form factor (SFF) in these models by going beyond the semiclassical periodic-orbit approaches [18,19]. These investigations have further strengthened our understanding of the *quantum chaos conjecture* [20–28] for describing the spectral fluctuations of many-body nonintegrable quantum systems by RMT. Until now, such microscopic derivation of SFF in many-body quantum models has been restricted to systems with single species, e.g., fermions, bosons, and qubits. Nature, however, is full of systems consisting of multiple species, such as the crystalline solids of electrons and phonons and the blackbody radiation comprising thermal electromagnetic radiation within or surrounding a matter in thermodynamic equilibrium. Inspired by these examples, we derive the leading-order contributions to SFF in various mixed many-body quantum systems with two different types of species, e.g., qubits and bosons or fermions [29].

We consider many-body quantum mixtures where a base Hamiltonian with the entries diagonal in the Fock space basis of two different species is kicked periodically by another Hamiltonian with terms consisting of mixing between two species and nearest-neighbor hopping of one species. The diagonal entries in the base Hamiltonian include random chemical potentials and transition frequencies along with pairwise long-range interactions of one species. We consider two forms of the mixing Hamiltonian: (a) Jaynes-Cummings (JC) [30–34] and (b) Rabi (R) [35,36] interaction between different species. While the JC preserves the total number of excitations of both species, the R does not. Thus, we have U(1) symmetry in the JC mixing system, which is absent for the R mixing. Our models' two different components are either qubit and spinless boson or qubit and spinless fermion. Since spinless fermions are related to spin-$1/2$'s or qubits, our results here are valid for many different types of mixtures, e.g., the results for a compound model of qubits and spinless bosons are also helpful for a mix between spinless fermions and bosons. Similarly, the results for a mixture of qubits and spinless fermions apply to a mixture of spin-$1/2$'s of different species, e.g., electrons and atomic nuclei in solids.

First, we rewrite the spectral form factor of the quantum mixtures in terms of a bistochastic many-body process [7,13] generated by an effective Hamiltonian. The effective Hamiltonian describes the leading-order contributions of SFF within the random phase approximation (RPA) in the Trotter regime of small perturbation parameters. We identify symmetries of the effective Hamiltonian controlling dynamical processes for the emergence of RMT behavior in these models [13,37]. These symmetries are important in determining system-size (L) scaling of the Thouless timescales t^* beyond which the SFF has a universal RMT-COE form for our time-reversal invariant models of a circular orthogonal ensemble (COE). For JC mixing, we find, $t^* \propto L^2$ when $L \to \infty$, which is a characteristics of a U(1)-symmetric model [5,7,13,38]. However, we show an exciting competition between the hopping and mixing of the driving Hamiltonian, leading to a crossover behavior in the L dependence of t^* when a finite-size system is considered. For a finite system, $t^* \propto \ln L$ when the mixing strength is smaller than the hopping, and $t^* \propto L^2$ for a higher mixing strength compared to hopping. The above crossover in L scaling of t^* is inevitable in many experimental studies with highly controlled laboratory settings of finite size [17,34,39–44]. For R mixing between fermions and qubits, $t^* \propto \ln L$ or L^0 for large L, which is similar to the single species of fermion or spin-$1/2$ models in the absence of U(1) symmetry. In contrast to fermions or spin-$1/2$'s, the only boson model lacking U(1) symmetry shows an algebraic L dependence of t^* [13]. We offer numerical evidence that the L dependence of t^* for R mixing between bosons and qubits seems to behave similarly to R mixing between fermions and qubits.

The base (kicked) Hamiltonian $\hat{H}_0$ of our systems denotes a one-dimensional lattice of length L consisting of spinless fermions or bosons and qubits with no coupling between these two species,

$$\hat{H}_0 = \sum_{i=1}^{L}(\omega_i \hat{n}_i + \Omega_i \hat{\sigma}_i^\dagger \hat{\sigma}_i) + \sum_{i<j} U_{ij}\hat{n}_i\hat{n}_j, \quad (1)$$

where $\hat{n}_i = \hat{a}_i^\dagger \hat{a}_i$ is the number operator, with $\hat{a}_i^\dagger$ being a fermion or boson creation operator at site i. We set $\hbar = 1$. The raising and lowering operators $\hat{\sigma}_j^\dagger \equiv (\hat{\sigma}_j^x + i\hat{\sigma}_j^y)/2$, $\hat{\sigma}_j \equiv (\hat{\sigma}_j^x - i\hat{\sigma}_j^y)/2$ are for the qubit at site j. Here, ω_i and Ω_i are, respectively, on-site energy of the fermion or boson and the transition frequency of the qubit at site i. We choose one or both of ω_i and Ω_i random as Gaussian independent and identically distributed (iid) variables of zero mean and finite standard deviation. We further take long-range interaction between fermions or bosons at sites i and j given by $U_{ij} = U_0/|i-j|^\alpha$ with an exponent in the interval $1 < \alpha < 2$. The form of $\hat{H}_0$ is fixed by minimal requirements for analytical calculation as well as physical relevance. Our analytical calculation requires the RPA and integration out of the parameters of $\hat{H}_0$, and both are met by the above choice of $\hat{H}_0$. The model with bosons and qubits and its close variants can physically represent light-matter interactions in real systems and engineered metamaterials [31,34,36] and electron-phonon interactions in crystalline solids.

The driving Hamiltonian consists of a term denoting the mixing between fermions or bosons and qubits locally and another term indicating nearest-neighbor hopping of fermions or bosons. The driving Hamiltonians with JC and R interactions are, respectively,

$$\hat{H}_{\rm JC} = \sum_{i=1}^{L} g(\hat{a}_i^\dagger \hat{\sigma}_i + \hat{\sigma}_i^\dagger \hat{a}_i) + \sum_{i=1}^{L}(-J\hat{a}_i^\dagger \hat{a}_{i+1} + \text{H.c.}), \quad (2)$$

$$\hat{H}_{\rm R} = \sum_{i=1}^{L} g(\hat{a}_i^\dagger + \hat{a}_i)(\hat{\sigma}_i + \hat{\sigma}_i^\dagger) + \sum_{i=1}^{L}(-J\hat{a}_i^\dagger \hat{a}_{i+1} + \text{H.c.}), \quad (3)$$

where g and J are the strength of mixing and hopping. The total excitation number operator, $\hat{N} = \sum_{i=1}^{L}(\hat{n}_i + \hat{\sigma}_i^\dagger \hat{\sigma}_i)$, commutes with both $\hat{H}_0$ and $\hat{H}_{\rm JC}$, but not with $\hat{H}_{\rm R}$. Thus, the time-dependent total Hamiltonian, $\hat{H}(t) = \hat{H}_0 + \hat{H}_{\rm JC/R}\sum_{m\in\mathbb{Z}}\delta(t-m)$, commutes with $\hat{N}$ for JC interaction, but not for R interaction, showing the presence or absence of a U(1) symmetry, which corresponds, respectively, to conservation or violation of the total excitation number in our models. Here we use the periodic boundary condition (PBC) in real space, i.e., $\hat{a}_i \equiv \hat{a}_{i+L}, \hat{\sigma}_i \equiv \hat{\sigma}_{i+L}$.

The SFF, $K(t)$, is defined as a time (t) Fourier transformation of the two-point correlation of the spectral density of quasienergies, which are eigenvalues of the unitary one-cycle Floquet propagator $\hat{U}$ of our periodically driven systems. $K(t)$ can be written as [1,7]

$$K(t) = \langle(\text{tr}\hat{U}^t)(\text{tr}\hat{U}^{-t})\rangle - \left(\mathcal{N}_\zeta^\beta\right)^2\delta_{t,0}, \quad (4)$$

where $\mathcal{N}_\zeta^\beta$ is the dimension of the Hilbert space of the system with $\zeta = $ JC, R mixing for fermions ($\beta = F$) and bosons ($\beta = B$). Here, $\langle\cdot\rangle$ denotes an average over the quench disorders $\{\Omega_i\}$ and/or $\{\omega_i\}$. The one-cycle time-evolution operator $\hat{U}$ can be expressed as

$$\hat{U} = \hat{V}\hat{W}, \quad \hat{W} = e^{-i\hat{H}_0}, \text{ and } \hat{V} = e^{-i\hat{H}_{\rm JC/R}}. \quad (5)$$

We consider the basis states $|\underline{n\sigma}\rangle \equiv |n_1, \dots, n_L\rangle \otimes |\sigma_1, \dots, \sigma_L\rangle$, where the occupation number of spinless fermion or boson and qubit at the lattice site j is, respectively, given by $n_j = 0, 1\,(F)$ and $0, 1, 2, \dots (B)$, and $\sigma_j = 0, 1$. The total number of excitations, $N \equiv \langle\underline{n\sigma}|\hat{N}|\underline{n\sigma}\rangle = \sum_{j=1}^{L}(n_j + \sigma_j)$, is conserved in the whole system only for JC mixing.

For JC mixing of fermions and qubits, we can distribute total excitations $N(< 2L)$ among $2L$ states consisting of L spatially localized qubit excitations and another L spatially delocalized fermionic excitations. Thus, the dimension of the Hilbert space for this system with N excitations is $\mathcal{N}_{\rm JC}^{\rm F} = (2L)!/[(2L-N)!N!]$. We further have, $\mathcal{N}_{\rm R}^{\rm F} = \sum_{N=0,2,\dots}^{2L}\mathcal{N}_{\rm JC}^{\rm F} = 2^{2L-1}$, which is the dimension of the Hilbert space for R mixing of fermions and qubits with even number of total excitations.

For JC mixing between bosons and qubits, the number of qubit excitations, M ($\equiv \sum_{j=1}^{L}\sigma_j$), can be $0 \leqslant M \leqslant \min(N, L)$. The total number of bosons there would be $N - M$. We can find the dimension $\mathcal{N}_{\rm JC}^{\rm B}$ of the Hilbert space by summing over allowed M. Thus, we get

$$\mathcal{N}_{\rm JC}^{\rm B} = \sum_{M=0}^{\min(N,L)} \frac{L!}{M!(L-M)!}\frac{(N-M+L-1)!}{(N-M)!(L-1)!}. \quad (6)$$

The Hilbert space dimension $\mathcal{N}_{\rm R}^{\rm B}$ becomes infinite for R mixing of bosons and qubits as N is not conserved and has no upper bound. However, as discussed later, it is possible to introduce a truncation for a maximum number of total excitation, $N_{\rm max}$, in the lattice for numerical calculation.

Both for fermionic and bosonic models, these basis states $|\underline{n\sigma}\rangle$ are eigenstates of $\hat{H}_0$ and $\hat{W}$, which allows us to integrate out $\hat{H}_0$ from $\hat{U}$ and $K(t)$ through the RPA by disorder averaging over different realizations. We further make an identity permutation approximation to achieve the following simple form of the SFF [7,13] by including the leading-order contributions at times $t \ll t_{\rm H} \equiv \mathcal{N}_\zeta^\beta$: $K(t) = 2t\,\text{tr}\mathcal{M}^t$, where $\mathcal{M}$ is a $\mathcal{N}_\zeta^\beta \times \mathcal{N}_\zeta^\beta$ double-stochastic square matrix whose elements are $\mathcal{M}_{\underline{n\sigma},\underline{n\sigma}'} = |\langle\underline{n\sigma}|\hat{V}|\underline{n\sigma}'\rangle|^2$. The largest eigenvalue of $\mathcal{M}$ is one. Thus, we can write the eigenvalues of $\mathcal{M}$ as $1, \lambda_1, \lambda_2, \lambda_3, \dots$, with $1 \geqslant |\lambda_i| \geqslant |\lambda_{i+1}|$. Using these eigenvalues, we express the SFF as (see Supplemental Material [45])

$$K(t) = 2t\left(1 + \sum_{i=1}^{\mathcal{N}_\zeta^\beta - 1}\lambda_i^t\right), \quad (7)$$

where $K(t) \simeq 2t$ is a leading order in the $t/t_{\rm H}$ result of RMT-COE. The RMT-COE form of $K(t) \simeq 2t$ in a leading order appears beyond the Thouless timescales $t^*(L)$ when the contribution from the second term in Eq. (7) becomes negligible. The contribution from the second term depends on the properties of λ_i for $i \geqslant 1$. We next try to understand the features of $\mathcal{M}$ and its eigenvalues. We can find Hermitian quantum Hamiltonians generating $\mathcal{M}$ in the Trotter regime of small g, J

for fermionic and bosonic models with JC and R mixing. The Hamiltonians are derived by writing $\mathcal{M}$ using an elementwise commutative product (also known as the Hadamard product) of $\hat{V}$ with $\hat{V}^*$ in the basis $|\underline{n\sigma}\rangle$, and then expanding $\hat{V}$ in the Trotter regime of small parameters of $\hat{H}_{\rm JC}$ ($\hat{H}_{\rm R}$) up to second order in $\hat{H}_{\rm JC}$ ($\hat{H}_{\rm R}$). The emergent symmetries of these generating Hamiltonians control the dynamical properties of these models, such as $t^*(L)$, and they can be significantly different from the symmetries of $\hat{H}(t)$.

We first analyze $\mathcal{M}$ for the fermionic model with JC mixing. The generating Hamiltonian for the PBC is (see Supplemental Material [45])

$$\mathcal{M}_{\rm JC}^{\rm F} = \left(1 - \frac{(g^2+J^2)L}{2}\right)\mathbb{1}_{\mathcal{N}_{\rm JC}^{\rm F}} + \sum_{i=1}^{L}\sum_{\nu}\left(\frac{J^2}{2}\hat{\tau}_i^{\nu}\hat{\tau}_{i+1}^{\nu} + \frac{g^2}{2}\hat{\tau}_i^{\nu}\hat{\sigma}_i^{\nu}\right) + \mathcal{O}(J^4, g^4), \tag{8}$$

where $\hat{\tau}_i^{\nu}$ and $\hat{\sigma}_i^{\nu}$ are the νth component of the Pauli matrix at site i and $\nu \in \{x, y, z\}$. Here, $\hat{\tau}_i^{\nu}$ and $\hat{\sigma}_i^{\nu}$ represent, respectively, the spinless fermions and qubits. The largest eigenvalue one of $\mathcal{M}_{\rm JC}^{\rm F}$ corresponds to a state in which all τ and σ spins are polarized in one particular direction, say along the z axis. $\mathcal{M}_{\rm JC}^{\rm F}$ commutes with the operators, $\sum_{j=1}^{L}(\hat{\tau}_j^{\nu} + \hat{\sigma}_j^{\nu})/2$, for $\nu \in \{x, y, z\}$, which satisfy the SU(2) algebra. Thus, $\mathcal{M}_{\rm JC}^{\rm F}$ has SU(2) symmetry, which implies that there would be degenerate symmetry multiplets of the subleading eigenvalues of $\mathcal{M}_{\rm JC}^{\rm F}$ for different N $(= 1, 2, 3, \dots, 2L-1)$. Nevertheless, other energy eigenvalues can also appear between different descendent states for higher N. Since we are interested in the L dependence of t^* at finite filling fractions (N/L), the ordering of descendant states in the full spectrum of $\mathcal{M}_{\rm JC}^{\rm F}$ for $N > 1$ is important. It can be shown that the value of λ_1 is the same for all N, including $N = 1$ at any value of g, J. The largest $L-1$ eigenvalues of $\mathcal{M}_{\rm JC}^{\rm F}$ excluding the largest eigenvalue one for $N = 1$ are

$$\lambda_i = 1 - g^2 - J^2\left(1 - \cos\frac{2i\pi}{L}\right) + \sqrt{J^4\left(1 - \cos\frac{2i\pi}{L}\right)^2 + g^4}, \tag{9}$$

for $i = 1, 2, 3 \dots, L-1$. We show below that the degeneracies of the λ_i's, which information is essential in determining the L scaling of t^*, can be different depending on the ratio of g/J.

In the thermodynamic limit of $L \to \infty$, the second-largest eigenvalues (λ_1) are doubly degenerate due to reflection symmetry, and can be approximated as $\lambda_1 \approx 1 - (2\pi^2 J^2)/L^2$ from Eq. (9) for any value of g, J. However, the above is also true for a finite but large L when $(1 - \cos\frac{2\pi}{L}) \ll (g/J)^2$, which requires $L > l_c \equiv \pi/\sin^{-1}(g/\sqrt{2}J)$. Here, l_c is a critical length scale. We then further approximate $K(t)$ at long time t, $1 \ll t \ll \mathcal{N}_{\rm JC}^{\rm F}$, by keeping up to the second-largest eigenvalues λ_1 of $\mathcal{M}_{\rm JC}^{\rm F}$. Thus, we get, for SFF,

$$K(t) \simeq 2t\left(1 + 2\lambda_1^t\right) \simeq 2t\left(1 + 2e^{-t/t^*(L)}\right), \tag{10}$$

where we take the scaling of λ_1 with system size L as $1 - 1/t^*$ and $t^* = L^2/(2\pi^2 J^2)$ [7,13]. The above L dependence of t^* is similar to our earlier result in Ref. [7] for a U(1) symmetric fermionic model without the qubits.

However, there is another interesting parameter regime when $(1 - \cos\frac{2i\pi}{L}) \gg (g/J)^2$ for a finite L, which is the case in many proposed highly controlled laboratory settings to test predictions for SFF [17,42–44,46]. For $(1 - \cos\frac{2i\pi}{L}) \gg (g/J)^2$ at finite L $(< l_c)$, we have, from Eq. (9),

$$\lambda_i \approx 1 - g^2 + \left(\frac{g^2}{2J}\right)^2 \csc^2\left(\frac{i\pi}{L}\right) \quad \text{for} \quad i = 1, 2, 3 \dots, L-1. \tag{11}$$

Therefore, the second-largest eigenvalues for small g/J are approximately $(L-1)$-fold degenerate. This degeneracy can be understood from first-order degenerate perturbation theory. When $g = 0$, the largest eigenvalues of one are L-fold degenerate. This degeneracy is lifted when a small but nonzero mixing g is introduced. It results in the largest eigenvalue of one and $(L-1)$-fold degenerate second-largest eigenvalues of $1 - g^2$. It can also be shown that these eigenvalues are independent of N in this case (see Supplemental Material [45]). These features of λ_i give a different form of SFF and the system-size scaling of t^*:

$$K(t) \simeq 2t\left(1 + \sum_{i=1}^{L-1}\lambda_i^t\right), \tag{12}$$

which leads to $t^* \approx \mathcal{O}(\ln L)$ (see Supplemental Material [45]). Such logarithmic system-size dependence of t^* has been previously reported for U(1) symmetry-broken models without total particle number conservation [1]. We can also increase the value of g/J at a fixed finite L to access the other condition, $(1 - \cos\frac{2i\pi}{L}) \ll (g/J)^2$, to get the SFF in Eq. (10), and $t^* \propto L^2$. Thus, we find a crossover in system-size scaling of t^* with a varying scaled mixing strength g/J at finite lengths in our model with JC mixing between fermions and qubits. We show in the Supplemental Material [45] that such crossover can also be observed in a periodically kicked quantum mixture of three species.

To demonstrate two different L scaling of t^*, we plot $K(t)$ with t using Eq. (7), which is obtained by applying the RPA and identity permutation for leading-order contributions. In Figs. 1(a) and 1(c), we show $K(t)$ with t for $g = 0.1, J = 0.4$ $(l_c \sim 17)$ and $g = 0.4, J = 0.1$ $(l_c \sim 0)$, respectively. We take the half-filled case with $N/L = 1/2$. We can understand the L dependence of t^* for these two parameter sets by scaling t and $K(t)$ by predicted L dependence. For this, we plot $K(t)/\ln L$ against $t/\ln L$ in Fig. 1(b) and $K(t)/L^{1.85}$ against $t/L^{1.85}$ in Fig. 1(d). Figures 1(b) and 1(d) display a nice data collapse for different L at a time above t^* for the universal RMT behavior of the SFF. Such data collapse confirms our above-predicted crossover of the L dependence of t^* with an increasing g/J. We could not get t^* growing exactly as L^2 for a large g/J in our numerics with limited L. Still, our obtained exponent (~ 1.85) in this region is close to the predicted value of 2. In the Supplemental Material [45], we further demonstrate such crossover in system-size scaling of t^* by directly simulating $K(t)$ using Eq. (4) for JC mixing between fermions and qubits.

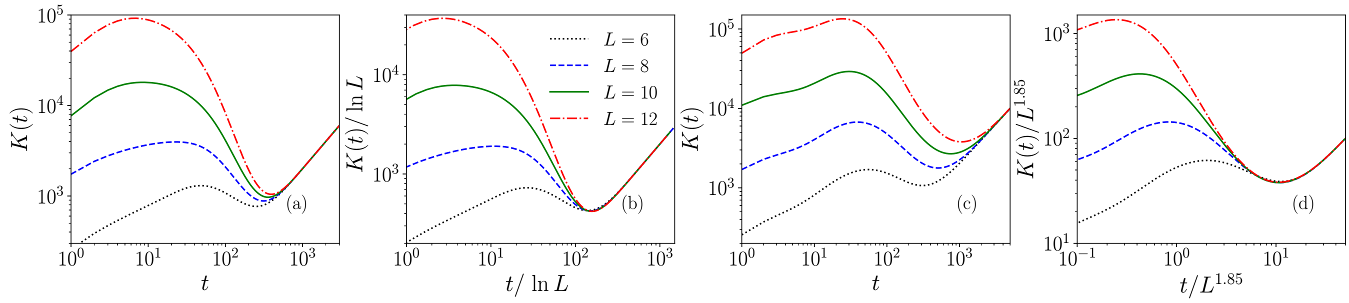

FIG. 1. Spectral form factor $K(t)$ using Eq. (7) for different system sizes L of the periodically kicked chain with JC mixing between fermions and qubits for (a),(b) $g = 0.1$, $J = 0.4$ and (c),(d) $g = 0.4$, $J = 0.1$. We take half filling $N/L = 1/2$. In (b) and (d), we show the data collapse in scaled time $t/\ln L$ and $t/L^{1.85}$, respectively.

The generating Hamiltonian for JC mixing between bosons and qubits in the Trotter regime reads as (see Supplemental Material [45])

$$\mathcal{M}^{\rm B}_{\rm JC} = \left(1 + \frac{(g^2+J^2)L}{2}\right)\mathbb{1}_{\mathcal{N}^{\rm B}_{\rm JC}} + \sum_{i=1}^{L}\big[2J^2\big(\hat{K}^1_i\hat{K}^1_{i+1} + \hat{K}^2_i\hat{K}^2_{i+1} - \hat{K}^0_i\hat{K}^0_{i+1}\big) + g^2\big(\hat{K}^1_i\hat{\sigma}^x_i - \hat{K}^2_i\hat{\sigma}^y_i + \hat{K}^0_i - \hat{\sigma}^\dagger_i\hat{\sigma}_i\big)\big] + \mathcal{O}(J^4, g^4), \quad (13)$$

where $\hat{K}^1_j = (\hat{K}^+_j + \hat{K}^-_j)/2$, $\hat{K}^2_j = (\hat{K}^+_j - \hat{K}^-_j)/2i$. We define a set of local operators $\hat{K}^0_j = -(\hat{n}_j + 1/2)$, $\hat{K}^+_j = \hat{a}_j\sqrt{\hat{n}_j}$, $\hat{K}^-_j = \sqrt{\hat{n}_j}\hat{a}^\dagger_j$, which satisfy the commutation relations of SU(1,1) algebra at the same site, and commute otherwise: $[\hat{K}^+_i, \hat{K}^-_j] = -2\hat{K}^0_i\delta_{ij}$, $[\hat{K}^0_i, \hat{K}^\pm_j] = \pm\hat{K}^\pm_i\delta_{ij}$. However, $\mathcal{M}^{\rm B}_{\rm JC}$ in Eq. (13) does not commute with $\hat{K}^\alpha = \sum_{i=1}^{L}\hat{K}^\alpha_i$, $\alpha \in \{+, -, 0\}$ for a nonzero g. Thus, $\mathcal{M}^{\rm B}_{\rm JC}$ does not possess SU(1,1) symmetry, unlike the only boson model investigated by Roy *et al.* [13]. Nevertheless, we find

$$\left[\mathcal{M}^{\rm B}_{\rm JC}, \sum_i\big(\hat{K}^0_i + \hat{\sigma}^\dagger_i\hat{\sigma}_i\big)\right] = 0, \quad (14)$$

which indicates a U(1) symmetry of $\mathcal{M}^{\rm B}_{\rm JC}$. As shown in the Supplemental Material [45], the L dependence of t^* for this model is similar to that of fermions and qubits. For a finite L, there is a crossover in the L dependence of t^* from $\ln L$ to L^2 with an increasing g/J for JC mixing between bosons and qubits. The eigenvalues of $\mathcal{M}^{\rm B}_{\rm JC}$ are identical to those of $\mathcal{M}^{\rm F}_{\rm JC}$ for $N = 1$. The largest eigenvalues of $\mathcal{M}^{\rm B}_{\rm JC}$ for any finite N become degenerate with those for $N = 1$ with an increasing L due to an emergent approximate symmetry of $\mathcal{M}^{\rm B}_{\rm JC}$. The above features lead to the similarity between the fermionic and bosonic models with JC mixing.

Next, we consider R mixing between fermions or bosons and qubits. We start with the fermionic case having a finite-dimensional Hilbert space. The generating Hamiltonian in this case is (see Supplemental Material [45])

$$\mathcal{M}^{\rm F}_{\rm R} = \left(1 - \frac{(2g^2+J^2)L}{2}\right)\mathbb{1}_{\mathcal{N}^{\rm F}_{\rm R}} + \sum_{i=1}^{L}\left(\sum_\nu \frac{J^2}{2}\hat{\tau}^\nu_i\hat{\tau}^\nu_{i+1} + g^2\hat{\tau}^z_i\hat{\sigma}^z_i\right) + \mathcal{O}(J^4, g^4), \quad (15)$$

which commutes with $\sum_{i=1}^{L}\hat{\tau}^z_i$ and $\hat{\sigma}^z_j$ for $j \in \{1, 2, 3, \dots, L\}$, indicating a global U(1) symmetry for fermions and local U(1) symmetry for each qubit. Interestingly, $\hat{H}(t)$ does not have a global U(1) symmetry for R mixing. The generating Hamiltonian for R mixing does not have SU(2) symmetry due to magnetic anisotropy created by coupling to the qubits, in contrast to that in Eq. (8) for JC mixing between fermions and qubits. The eigenvalues λ_i of $\mathcal{M}^{\rm F}_{\rm R}$ can be determined by fixing $\sum_{i=1}^{L}\hat{\tau}^z_i$ and $\hat{\sigma}^z_j$ for $j \in \{1, 2, 3, \dots, L\}$ as these are good quantum numbers. The eigenvalues are doubly degenerate since $\mathcal{M}^{\rm F}_{\rm R}$ is invariant under $\prod_{i=1}^{L}\hat{\tau}^x_i\hat{\sigma}^x_i$, which implies that a state obtained by flipping all the τ and σ spins of an eigenstate of $\mathcal{M}^{\rm F}_{\rm R}$ is also an eigenstate with the same eigenvalue. The largest eigenvalue one of $\mathcal{M}^{\rm F}_{\rm R}$ is a state $|\lambda_0\rangle$ in which all τ and σ spins are polarized in the z direction. The second-largest eigenvalues of $\mathcal{M}^{\rm F}_{\rm R}$ are $(L+1)$- and L-fold degenerate, respectively, for $(g/J)^2 < 2/3$ and $(g/J)^2 > 2/3$ (see Supplemental Material [45]). For $(g/J)^2 < 2/3$, the second-largest eigenvalues are $1 - 2g^2$, which consist of L eigenstates with any one σ spin being flipped in $|\lambda_0\rangle$ and another superposition state with a single τ spin flipping in $|\lambda_0\rangle$. For $(g/J)^2 > 2/3$, the second-largest eigenvalues are $1 - 4g^2 - 2J^2[1 - \sqrt{1 + 4(g/J)^4}]$ [47], which are L eigenstates with one τ spin flipping and one σ spin being flipped in $|\lambda_0\rangle$. Thus, the second-largest eigenvalues for any g/J are L independent. So we get $t^* \propto \ln L$ or $\ln(L+1)$ for R mixing between fermions and qubits. Such L dependence of t^* is similar to that in a periodically kicked transverse-field Ising model in Kos *et al.* [1] with local kicking terms. Interestingly, a similar L scaling of t^* can also be obtained for the U(1)-symmetry-broken model explored in Ref. [7] when the pairing Δ and tunneling J strengths are the same. We can also get $t^* \propto L^0$ of Ref. [7] for arbitrary Δ and J when g is different (or random) for different qubits to lift the degeneracy in the second-largest eigenvalues.

Finally, we consider the mixture of bosons and qubits with R mixing between them. The generating Hamiltonian for this case in the Trotter regime reads as (see Supplemental Material [45])

$$\mathcal{M}^{\rm B}_{\rm R} = \left(1 + \frac{J^2L}{2}\right)\mathbb{1}_{\mathcal{N}^{\rm B}_{\rm R}} + \sum_{i=1}^{L}\big[2J^2\big(\hat{K}^1_i\hat{K}^1_{i+1} + \hat{K}^2_i\hat{K}^2_{i+1} - \hat{K}^0_i\hat{K}^0_{i+1}\big) + 2g^2\big(\hat{K}^1_i\hat{\sigma}^x_i + \hat{K}^0_i\big)\big] + \mathcal{O}(J^4, g^4), \quad (16)$$

which commutes with $\hat{\sigma}_j^x$ for $j \in \{1, 2, 3, \ldots, L\}$. We could not calculate the spectrum of $\mathcal{M}_{\mathrm{R}}^{\mathrm{B}}$ analytically. Instead, we determine it numerically by varying $N_{\max}$ for a fixed L to get an estimate of λ_1 in the large-$N_{\max}$ limit. We use linear extrapolations in $1/N_{\max}$ towards $1/N_{\max} = 0$ to find evidence for a gap between the largest and second-largest eigenvalues, as shown in the Supplemental Material [45]. The second-largest eigenvalues are also L-fold degenerate, suggesting a scaling of $t^* \propto \ln L$. We remind the reader here that a periodically kicked boson model without particle-number conservation shows $t^* \propto \mathcal{O}(L^\gamma)$, $\gamma = 0.7 \pm 0.1$ [13], which is sharply different from the present case of bosons and qubits without total-number conservation.

We have analytically calculated the SFF in many-body quantum mixtures of fermions, bosons, and qubits with periodically kicked spreading and mixing of species. Different types of mixing between species can drastically alter the timescale for the emergence of RMT behavior of $K(t)$ in quantum mixtures. We show how competition between mixing and spreading of species in U(1)-symmetric finite-size systems can lead to a logarithmic L scaling of t^*, which has been predicted before only for U(1)-symmetry-broken single-species models [1,4]. This finding is practical and vital as quantum mixtures of different species are abundant in nature as well as controlled experimental setups of cold atoms and photonic systems, and many of these systems are finite size. We further show that the t^* scaling for R mixing of fermions and qubits is similar to those obtained for a single species of spin-1/2′s or fermions. Finally, our results indicate that the R mixing of species with different statistics (e.g., bosons and qubits) can lead to completely different features for the main species (e.g., bosons) with individual hopping.

We thank Prof. Tomaž Prosen for many useful discussions.

[1] P. Kos, M. Ljubotina, and T. Prosen, Many-body quantum chaos: Analytic connection to random matrix theory, Phys. Rev. X **8**, 021062 (2018).

[2] B. Bertini, P. Kos, and T. Prosen, Exact spectral form factor in a minimal model of many-body quantum chaos, Phys. Rev. Lett. **121**, 264101 (2018).

[3] A. Chan, A. De Luca, and J. T. Chalker, Solution of a minimal model for many-body quantum chaos, Phys. Rev. X **8**, 041019 (2018).

[4] A. Chan, A. De Luca, and J. T. Chalker, Spectral statistics in spatially extended chaotic quantum many-body systems, Phys. Rev. Lett. **121**, 060601 (2018).

[5] A. J. Friedman, A. Chan, A. De Luca, and J. T. Chalker, Spectral statistics and many-body quantum chaos with conserved charge, Phys. Rev. Lett. **123**, 210603 (2019).

[6] B. Bertini, P. Kos, and T. Prosen, Exact correlation functions for dual-unitary lattice models in 1 + 1 dimensions, Phys. Rev. Lett. **123**, 210601 (2019).

[7] D. Roy and T. Prosen, Random matrix spectral form factor in kicked interacting fermionic chains, Phys. Rev. E **102**, 060202(R) (2020).

[8] B. Bertini, P. Kos, and T. Prosen, Random matrix spectral form factor of dual-unitary quantum circuits, Commun. Math. Phys. **387**, 597 (2021).

[9] S. J. Garratt and J. T. Chalker, Local pairing of feynman histories in many-body Floquet models, Phys. Rev. X **11**, 021051 (2021).

[10] J. Li, T. Prosen, and A. Chan, Spectral statistics of non-Hermitian matrices and dissipative quantum chaos, Phys. Rev. Lett. **127**, 170602 (2021).

[11] P. Kos, B. Bertini, and T. Prosen, Chaos and ergodicity in extended quantum systems with noisy driving, Phys. Rev. Lett. **126**, 190601 (2021).

[12] S. Moudgalya, A. Prem, D. A. Huse, and A. Chan, Spectral statistics in constrained many-body quantum chaotic systems, Phys. Rev. Res. **3**, 023176 (2021).

[13] D. Roy, D. Mishra, and T. Prosen, Spectral form factor in a minimal bosonic model of many-body quantum chaos, Phys. Rev. E **106**, 024208 (2022).

[14] M. Winer and B. Swingle, The Loschmidt spectral form factor, J. High Energy Phys. 10 (2022) 137.

[15] M. Winer and B. Swingle, Hydrodynamic theory of the connected spectral form factor, Phys. Rev. X **12**, 021009 (2022).

[16] Y. Liao and V. Galitski, Emergence of many-body quantum chaos via spontaneous breaking of unitarity, Phys. Rev. B **105**, L140202 (2022).

[17] C. B. Dağ, S. I. Mistakidis, A. Chan, and H. R. Sadeghpour, Many-body quantum chaos in stroboscopically driven cold atoms, Commun. Phys. **6**, 136 (2023).

[18] F. Haake, *Quantum Signatures of Chaos*, 2nd ed. (Springer, New York, 2001).

[19] M. V. Berry, Semiclassical theory of spectral rigidity, Proc. R. Soc. London A **400**, 229 (1985).

[20] O. Bohigas, M. J. Giannoni, and C. Schmit, Characterization of chaotic quantum spectra and universality of level fluctuation laws, Phys. Rev. Lett. **52**, 1 (1984).

[21] S. W. McDonald and A. N. Kaufman, Spectrum and eigenfunctions for a Hamiltonian with stochastic trajectories, Phys. Rev. Lett. **42**, 1189 (1979).

[22] G. Casati, F. Valz-Gris, and I. Guarnieri, On the connection between quantization of nonintegrable systems and statistical theory of spectra, Lett. Nuovo Cimento **28**, 279 (1980).

[23] M. V. Berry and M. Tabor, Level clustering in the regular spectrum, Proc. R. Soc. London A **356**, 375 (1977).

[24] M. V. Berry, Quantizing a classically ergodic system: Sinai′s billiard and the KKR method, Ann. Phys. **131**, 163 (1981).

[25] M. Sieber and K. Richter, Correlations between periodic orbits and their role in spectral statistics, Phys. Scr. **2001**, 128 (2001).

[26] M. Sieber, Leading off-diagonal approximation for the spectral form factor for uniformly hyperbolic systems, J. Phys. A: Math. Gen. **35**, L613 (2002).

[27] S. Müller, S. Heusler, P. Braun, F. Haake, and A. Altland, Semiclassical foundation of universality in quantum chaos, Phys. Rev. Lett. **93**, 014103 (2004).

[28] S. Müller, S. Heusler, P. Braun, F. Haake, and A. Altland, Periodic-orbit theory of universality in quantum chaos, Phys. Rev. E **72**, 046207 (2005).

[29] J. Chávez-Carlos, B. López-del-Carpio, M. A. Bastarrachea-Magnani, P. Stránský, S. Lerma-Hernández, L. F. Santos, and J. G. Hirsch, Quantum and classical Lyapunov exponents in atom-field interaction systems, Phys. Rev. Lett. **122**, 024101 (2019).

[30] E. T. Jaynes and F. W. Cummings, Comparison of quantum and semiclassical radiation theories with application to the beam maser, Proc. IEEE. **51**, 89 (1963).

[31] M. Scully and M. Zubairy, *Quantum Optics* (Cambridge University Press, Cambridge, 1997).

[32] M. J. Hartmann, F. G. S. L. Brandão, and M. B. Plenio, Strongly interacting polaritons in coupled arrays of cavities, Nat. Phys. **2**, 849 (2006).

[33] D. G. Angelakis, M. F. Santos, and S. Bose, Photon-blockade-induced Mott transitions and XY spin models in coupled cavity arrays, Phys. Rev. A **76**, 031805(R) (2007).

[34] D. Roy, C. M. Wilson, and O. Firstenberg, *Colloquium*: Strongly interacting photons in one-dimensional continuum, Rev. Mod. Phys. **89**, 021001 (2017).

[35] I. I. Rabi, Space quantization in a gyrating magnetic field, Phys. Rev. **51**, 652 (1937).

[36] Q. Xie, H. Zhong, M. T. Batchelor, and C. Lee, The quantum Rabi model: Solution and dynamics, J. Phys. A: Math. Theor. **50**, 113001 (2017).

[37] L. Agarwal, S. Sahu, and S. Xu, Charge transport, information scrambling and quantum operator-coherence in a many-body system with U(1) symmetry, J. High Energy Phys. 05 (2023) 037.

[38] H. Gharibyan, M. Hanada, S. H. Shenker, and M. Tezuka, Onset of random matrix behavior in scrambling systems, J. High Energy Phys. 07 (2018) 124.

[39] R. Islam, R. Ma, P. M. Preiss, M. E. Tai, A. Lukin, M. Rispoli, and M. Greiner, Measuring entanglement entropy in a quantum many-body system, Nature (London) **528**, 77 (2015).

[40] A. M. Kaufman, M. E. Tai, A. Lukin, M. Rispoli, R. Schittko, P. M. Preiss, and M. Greiner, Quantum thermalization through entanglement in an isolated many-body system, Science **353**, 794 (2016).

[41] H. Bernien, S. Schwartz, A. Keesling, H. Levine, A. Omran, H. Pichler, S. Choi, A. S. Zibrov, M. Endres, M. Greiner, V. Vuletić, and M. D. Lukin, Probing many-body dynamics on a 51-atom quantum simulator, Nature (London) **551**, 579 (2017).

[42] S. Cronenberger, C. Abbas, D. Scalbert, and H. Boukari, Spatiotemporal spin noise spectroscopy, Phys. Rev. Lett. **123**, 017401 (2019).

[43] M. Swar, D. Roy, S. Bhar, S. Roy, and S. Chaudhuri, Detection of spin coherence in cold atoms via Faraday rotation fluctuations, Phys. Rev. Res. **3**, 043171 (2021).

[44] L. K. Joshi, A. Elben, A. Vikram, B. Vermersch, V. Galitski, and P. Zoller, Probing many-body quantum chaos with quantum simulators, Phys. Rev. X **12**, 011018 (2022).

[45] See Supplemental Material at http://link.aps.org/supplemental/10.1103/PhysRevE.109.L032201 for the derivation of the spectral form factor and generating Hamiltonians for different mixing, and the details of the spectral properties of these Hamiltonians in the Trotter regime.

[46] D. Roy, R. Singh, and R. Moessner, Probing many-body localization by spin noise spectroscopy, Phys. Rev. B **92**, 180205(R) (2015).

[47] E. N. Economou, *Green's Functions in Quantum Physics* (Springer Science & Business Media, New York, 2006), Vol. 7.